

Pentacene Appended to a TEMPO Stable Free Radical: The Effect of Magnetic Exchange Coupling on Photoexcited Pentacene

Erin T. Chernick,[†] Rubén Casillas,[‡] Johannes Zirzmeier,[‡] Daniel M. Gardner,[§] Marco Gruber,[†] Henning Kropp,^{||} Karsten Meyer,^{||} Michael R. Wasielewski,^{*,§} Dirk M. Guldi,^{*,‡} and Rik R. Tykwinski^{*,†}

[†]Department of Chemistry and Pharmacy & Interdisciplinary Center for Molecular Materials (ICMM), Friedrich-Alexander-Universität Erlangen-Nürnberg, Henkestr. 42, 91054 Erlangen, Germany

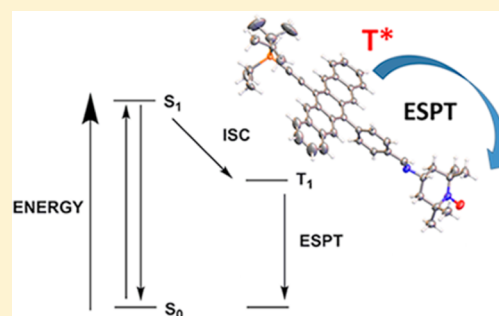
[‡]Chair of Physical Chemistry I & Interdisciplinary Center for Molecular Materials (ICMM), Friedrich-Alexander-Universität Erlangen-Nürnberg, Egerlandstr. 3, 91058 Erlangen, Germany

[§]Department of Chemistry and Argonne-Northwestern Solar Energy Research (ANSER) Center, Northwestern University, Evanston, Illinois 60208-3113, United States

^{||}Department of Chemistry and Pharmacy, Friedrich-Alexander-Universität Erlangen-Nürnberg, Egerlandstr. 1, 91058 Erlangen, Germany

S Supporting Information

ABSTRACT: Understanding the fundamental spin dynamics of photoexcited pentacene derivatives is important in order to maximize their potential for optoelectronic applications. Herein, we report on the synthesis of two pentacene derivatives that are functionalized with the [(2,2,6,6-tetramethylpiperidin-1-yl)oxy] (TEMPO) stable free radical. The presence of TEMPO does not quench the pentacene singlet excited state, but does quench the photoexcited triplet excited state as a function of TEMPO-to-pentacene distance. Time-resolved electron paramagnetic resonance experiments confirm that triplet quenching is accompanied by electron spin polarization transfer from the pentacene excited state to the TEMPO doublet state in the weak coupling regime.



Acenes are molecules formed from linearly fused benzene rings. As a result of their rather unique π -electron systems, acenes show a variety of interesting physical and optoelectronic properties. Significant effort has been devoted toward extending the length of the acene unit to decrease the HOMO–LUMO gap, which might improve performance in device applications.^{1–6} Attempts to synthesize longer acenes, however, have demonstrated a drastic decrease in stability beyond the size of pentacene (five fused rings).^{7–13} It has been reported that one reason for the instability of larger acenes is the open shell character of their ground state, suggesting that radical character might play an important role in the future of this class of compounds.^{3,14}

Pentacene and its derivatives offer a potential compromise between stability and desirable properties and have thus received a disproportionate amount of the attention as small molecule semiconductors for photophysical applications.^{15–17} The pentacene skeleton can be easily decorated with a variety of functional groups, which provide opportunities to explore and tune the structure,^{18–22} function,²³ stability,^{24,25} and processability.^{2,4,26}

From a photophysical perspective, excitation of a pentacene-based chromophore gives a singlet excited state, which has the potential to transform to the triplet excited state through the spin-selective process of intersystem crossing (ISC). While ISC

has been investigated for pentacene derivatives in the solid state,^{27,28} the same level of understanding of excited state dynamics has not yet been achieved in solution, where intermolecular interactions and photochemical processes are diffusion limited. Hence, it is clearly essential to develop a fundamental understanding of the spin dynamics of photoexcited pentacene derivatives in solution, in order to optimize and customize such materials for optoelectronic applications.

A simple and effective way to explore the spin dynamics of an excited chromophore without greatly perturbing its excited state energies is to introduce an unpaired spin in the form of a stable free radical.²⁹ It has been thoroughly documented that an unpaired electron spin enhances the ISC process, which is termed enhanced intersystem crossing (EISC) or spin catalysis.³⁰ This concept offers an opportunity to explore the spin dynamics of photoexcited pentacene derivatives, via incorporation of a stable radical group pendent to the acene chromophore. To probe this hypothesis, we envision a series of pentacene derivatives with the TEMPO free radical appended from the 13-position, opposite to the triisopropylsilylethynyl group in the 6-position. Two pentacene-TEMPO dyads have thus been targeted, **Ra** and **Rb**, along with two “nonradical”

Received: October 24, 2014

Published: December 5, 2014

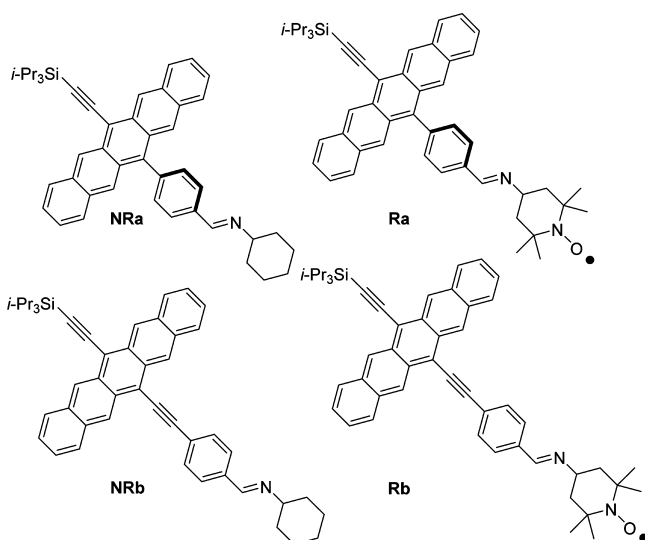


Figure 1. Pentacenes featuring a TEMPO free radical linked via an imine bond to a “nonplanar” phenyl spacer (**Ra**) and a “planar” phenylethynyl spacer (**Rb**); the structures of reference compounds, imines **NRa** and **NRb**.

reference compounds, **NRa** and **NRb** (Figure 1). The two pairs of pentacene derivatives **Ra/NRa** and **Rb/NRb** are designed with and without an alkyne spacer, respectively, so that the impact of the TEMPO free radical on pentacene in the ground and excited state can be evaluated based on two factors: (1) the overall distance of the radical from the pentacene framework and (2) molecular geometry, i.e., either a conjugated, planar arrangement of the phenyl ring to the pentacene core attached via the ethynyl spacer (**Rb/NRb**) or a nonplanar arrangement, where the phenyl ring is perpendicular (decoupled) to the pentacene core due to steric hindrance (**Ra/NRa**).

During the course of our studies, Teki and co-workers reported on the synthesis and characterization of pentacene derivatives covalently linked to conjugated stable free radicals and observed increased photostability. These pentacene derivatives were studied via time-resolved pump–probe spectroscopy and time-resolved electron paramagnetic resonance (EPR) spectroscopy. This report showed enhanced intersystem crossing (EISC), quartet state population due to strong spin–spin exchange coupling between the stable free radical and pentacene, and singlet fission (SF).^{31,32} The intriguing results from Teki and co-workers offer a significant basis for comparison for the photophysical behavior of **Ra** and **Rb**.

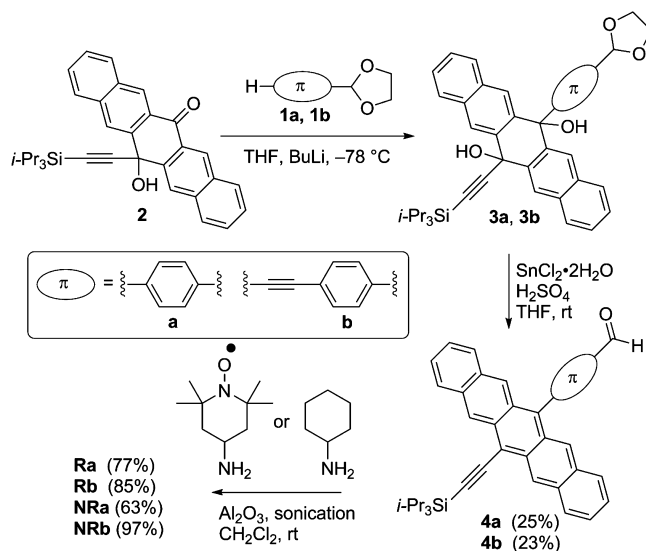
Based on the synthesis and study of **Ra/NRa** and **Rb/NRb**, we demonstrate in this report that the pentacene excited state can be *selectively* influenced by an unconjugated TEMPO stable free radical, where the spin–spin exchange couplings between the excited state and the radical are in the weak spin–spin exchange coupling regime. This result is particularly important because it presents the possibility that stable free radicals may be used to control the photoexcited spin states in organic molecules based on manipulating the magnitude of the magnetic-exchange interaction via the extent of conjugation with, and the distance from, a stable free radical.

RESULTS AND DISCUSSION

Synthesis. The synthesis of all four pentacene derivatives followed a similar route, beginning with addition of either

lithiated **1a**³³ or **1b**³⁴ to ketone **2**^{35,36} (Scheme 1). In each case, the requisite aldehyde groups of the aryl (**1a**)³⁷ or acetylide

Scheme 1. Synthesis of Pentacene Radicals **Ra** and **Rb** and Model Compounds **NRa** and **NRb**



(**1b**)^{38,39} moieties were protected as the corresponding acetals. Addition of the aryl lithium or lithiated acetylide gave diols **3a** and **3b**, which were then subjected to reductive aromatization in the presence of acid and $\text{SnCl}_2 \cdot 2\text{H}_2\text{O}$. These conditions concurrently removed the acetal protecting group to give directly **4a** and **4b**. The aldehyde functional groups of **4a** and **4b** provided a convenient synthetic handle for introducing either the TEMPO or cyclohexyl moiety based on imine formation using a procedure introduced by Stefani and co-workers.⁴⁰ Briefly, pentacene aldehydes **4a** and **4b** were subjected to sonication in the presence of alumina gel with either excess 4-amino-TEMPO or cyclohexylamine, in the absence of light. The alumina gel was removed by filtration, and the resulting product precipitated from the reaction mixture by addition of MeOH. This protocol gave radicals **Ra** and **Rb** in yields of 77% and 85%. Model compounds **NRa** and **NRb** in 63% and 97%, respectively, using the same general protocol.⁴¹

A crystal of **Ra** suitable for X-ray crystallographic analysis was grown at rt by slow evaporation of a CH_2Cl_2 solution layered with acetone. The molecular structure confirms the decoupling of the pendent TEMPO fragment and the pentacene core, via the orthogonal phenyl bridge (Figure 2). The packing of **Ra** shows π -stacking only between two neighboring molecules, arranged in centrosymmetric “dimeric pairs” with no long-range stacking.

Photophysical Characterization. Ground-state electronic properties have been probed by means of steady-state UV/vis absorption spectroscopy, and the most important values are summarized in Table 1. Compounds **Ra** and **NRa** show similar absorption maxima of $\lambda_{\text{abs}} = 620\text{--}621$ nm indicating little, if any, electronic communication between the pendent substituents and the pentacene skeleton in the ground state. On the other hand, **Rb** and **NRb** show red-shifted absorptions ($\lambda_{\text{abs}} = 656$ nm) compared to **Ra** and **NRa**, due to extended conjugation through the acetylene spacer and a coplanar conformation between the pentacene and aryl rings.

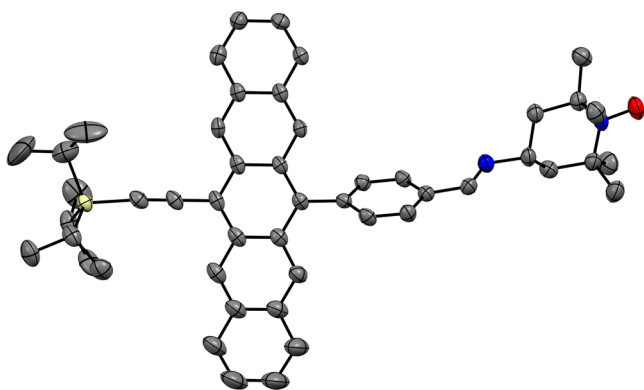


Figure 2. X-ray crystallographic structure of **Ra** illustrating the structure of the pendent TEMPO group and the pentacene chromophore (ORTEP drawn at 50% probability level; hydrogen atoms have been omitted for clarity).

Table 1. Summary of Photophysical Properties^a

compd	λ_{abs} (nm)	λ_{em} (nm)	Φ_{F} (%)	τ_{F} (ns)	τ_{ISC} (ns)
NRa	620	658	5.8 ± 0.4	6.6 ± 0.5	6.6 ± 0.1
Ra	621	658	6.2 ± 0.9	7.2 ± 0.03	7.1 ± 0.1
NRb	656	664	23.8 ± 0.7	11.2 ± 0.1	9.8 ± 0.1
Rb	656	665	25.3 ± 0.5	11.6 ± 0.4	9.6 ± 0.1

^aObtained at 0.1 mM (τ_{F} and τ_{ISC}) and 0.01 mM (λ_{abs} , λ_{em} , and Φ_{F}) in THF.

To shed light on the excited-state interactions, steady-state fluorescence measurements were performed on both the radical and nonradical species in THF with 610 nm photoexcitation. These experiments show fluorescence at 600–800 nm, with maxima and shoulders at ca. 660 and 725 nm, respectively, for all four compounds. From gradient analysis, fluorescence quantum yields (Φ_{F} , Figure 3 and Table 1) of 5.8 ± 0.4% for

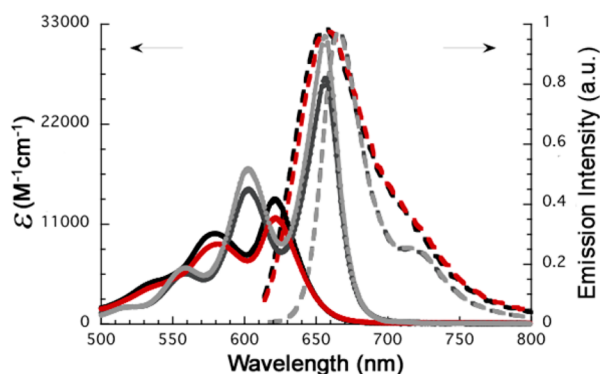


Figure 3. Absorption spectra (solid lines) of **NRa** (red), **Ra** (black), **NRb** (light gray), and **Rb** (dark gray) and fluorescence spectra (dashed lines) of **NRa** (red), **Ra** (black), **NRb** (light gray), and **Rb** (dark gray) recorded in THF; excitation wavelength of 610 nm.

NRa, 6.2 ± 0.9% for **Ra**, 23.8 ± 0.7% for **NRb**, and 25.3 ± 0.5% for **Rb** were determined. The fact that **NRb** and **Rb** have larger Φ_{F} values than **NRa** and **Ra** is consistent with the slower τ_{ISC} and longer τ_{F} observed for the former. The presence of the TEMPO radical has no appreciable impact on the fluorescence quantum yields. Fluorescence lifetime measurements (τ_{F}) are summarized in Table 1 and further corroborate the aforementioned trend. In particular, lifetimes measured for **NRa** and **NRb** with τ_{F} = 6.6 ± 0.5 and 11.2 ± 0.1 ns,

respectively, are nearly the same as those determined for **Ra** and **Rb** with τ_{F} = 7.2 ± 0.03 and 11.6 ± 0.4 ns, respectively.

Transient absorption (TA) pump probe experiments have been performed on **NRa**/**NRb** and **Ra**/**Rb** in THF (Figure 4).

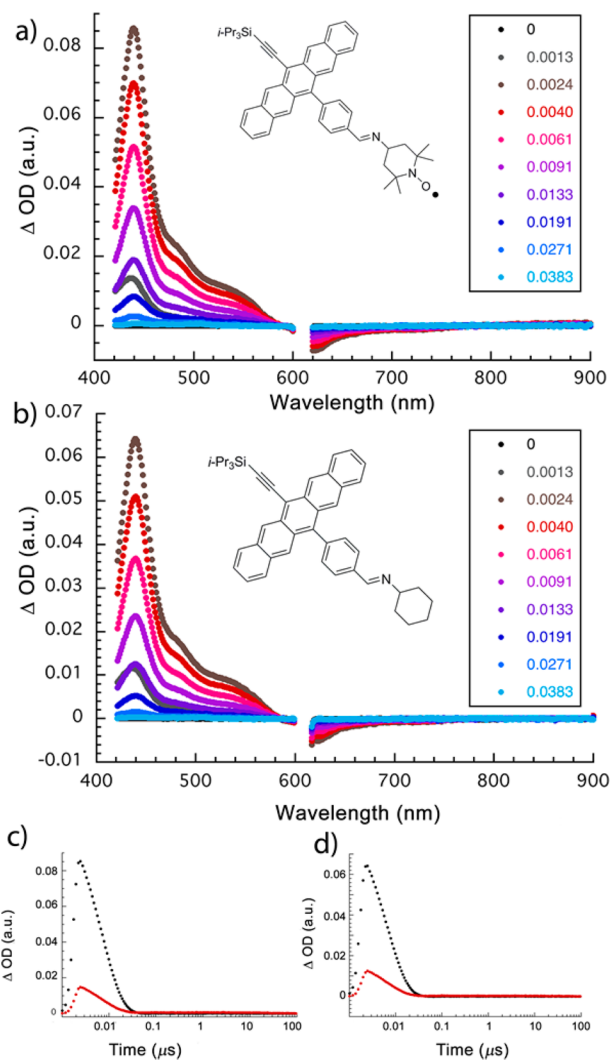


Figure 4. Differential absorption changes (visible) obtained upon femtosecond pump-probe experiments (610 nm) in THF saturated with argon for (a) **Ra** and (b) **NRa** at rt and with time delays between 0 and 0.0383 μs . Time absorption profiles at 438 (black) and 508 nm (red) monitoring the excited state dynamics for (c) **Ra** and (d) **NRa**.

All samples have been photoexcited at 610 nm to populate exclusively the first singlet excited states (S_1), and the differential absorption changes were recorded with delays on the 0.5 ps to 7.5 ns and 1 ns to 250 μs time scales (corresponding spectra are presenting in the Supporting Information (SI)). In the range of 0.5 ps to 7.5 ns after excitation, the differential absorption spectra are dominated by transients with maxima at 450, 510, 580, and 1225 nm and by bleaching with minima at 660 and 730 nm. The maxima in the visible and near-infrared are assigned to singlet–singlet transitions, while the minima in the visible reflect ground state bleaching and stimulated emission. Overall, the singlet-excited states of all samples are metastable and susceptible to a monoexponential, strict first-order ISC to afford the corresponding triplet states. From multiwavelength analyses, non-radiative ISC lifetimes (τ_{ISC} , Table 1) of τ_{ISC} = 6.6 ± 0.1, 9.8 ±

0.1, 7.1 ± 0.1 , and 9.6 ± 0.1 ns were determined for **NRa**, **NRb**, **Ra**, and **Rb**, respectively. The similar fluorescence lifetimes (τ_F), quantum yields (Φ_F), and ISC lifetimes (τ_{ISC}) observed for **Ra/Rb** and **NRa/NRb** suggest that TEMPO does not significantly influence the pentacene ISC process in these systems.

On the complementary time scale of 1 ns to 250 μ s, new differential absorption spectra evolve. For example, at time delays of 15 ns the differential absorption spectra are composed of positive transients in the range up to 550 nm and beyond 700 nm (including maxima at 470, 500, and 780 nm), as well as negative transients in the range from 550 to 700 nm (including minima at 600 and 650 nm), indicating that the pentacene triplet state is formed.^{8,42,43} This is followed on the microsecond time scale by quantitative recovery of the singlet ground state with lifetimes in the range of μ s for **NRa** and **NRb** that is dominated by triplet–triplet annihilation with a second-order rate constant of about $10^8 \text{ M}^{-1} \text{ s}^{-1}$.

Turning to pump–probe experiments, performed on **Ra** and **Rb**, quenching of the corresponding triplet excited states is observed with no evidence of singlet fission (SF).⁴⁴ Considering the low triplet quantum yields and triplet extinction coefficients observed for **Ra** and **Rb** (ca. 10% and $150\,000 \text{ M}^{-1} \text{ cm}^{-1}$, respectively), we have focused on the indirect photoexcitation, via triplet sensitization experiments with a *N*-fulleropyrrolidine (*N*-MFP) to determine the rate of quenching (Figure 5). Diffusion controlled triplet excited-state energy transfer populates the triplet excited states of **Ra** and **Rb** with rate constants of around $10^9 \text{ M}^{-1} \text{ s}^{-1}$. From multiwavelength analyses, triplet lifetimes (τ_T) of $\tau_T = 35 \pm 1 \mu\text{s}$ for **Ra** and $8 \pm 0.5 \mu\text{s}$ for **Rb** relative to $\tau_T = 53 \pm 0.5 \mu\text{s}$ for **NRa** and $31 \pm 0.5 \mu\text{s}$ for **NRb** are determined. The difference between the triplet lifetimes of **Ra** and **Rb** shows that the triplet excited-state quenching mechanism appears to be dependent on the pentacene–TEMPO distance.

EPR Spectroscopy. Steady-state continuous wave (CW) and time-resolved (TR) electron paramagnetic resonance (EPR) experiments at X-band (9.5 GHz) have been conducted on the pairs **Ra/NRa** and **Rb/NRb**, in order to examine the triplet excited state and the quenching process. The steady-state CW EPR spectra of **Ra** and **Rb** at rt (in toluene solution) are shown in Figure 6a. Both spectra consist of three lines centered at $g = 2.0057$ resulting from hyperfine coupling of the unpaired electron with the nitroxide ^{14}N nucleus ($a_N = 1.5 \text{ mT}$). The intensity of the hyperfine lines decreases with M_I , which is indicative of a slower rotational correlation time.⁴⁵ At 85 K (Figure 6b), the TEMPO powder spectrum is observed due to hyperfine anisotropy and g -anisotropy in a randomly oriented spin system with rhombic symmetry.⁴⁶

TREPR spectra were obtained at 85 K following photoexcitation with a 7 ns, 590 nm laser pulse. The TREPR spectra of **NRa** and **NRb** (Figure 7) consist of a broad signal characteristic of a spin-polarized triplet excited state that decays on the microsecond time scale. The TREPR spectrum for a frozen butyronitrile solution of TIPS pentacene (**TIPSPn**)⁴⁷ was also obtained (Figure 7c), because no powder spectrum for the **TIPSPn** triplet excited state has yet been reported in the literature, although pentacene triplets have been studied extensively^{48–55} in host–guest crystals of *p*-terphenyl, naphthalene, and benzoic acid. All three compounds **NRa**, **NRb**, and **TIPSPn** yield identical spectra consisting of a broad feature with an *a,a,e,a,e,e* (*a* = enhanced absorption, *e* = emission) polarization pattern, consistent with a spin–orbit ISC

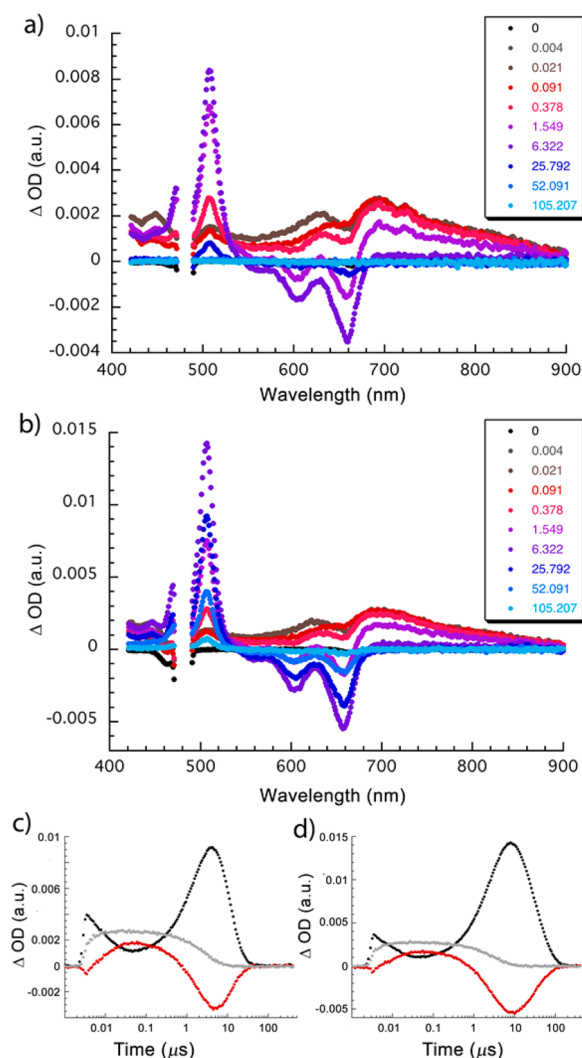


Figure 5. Differential absorption changes (visible) obtained upon femtosecond pump–probe experiments (480 nm) of a *N*-MFP ($8.0 \times 10^{-5} \text{ M}$) with (a) **Rb** and (b) **NRb** ($1.0 \times 10^{-4} \text{ M}$) in THF saturated with argon at rt with time delays between 0 and 105 μ s. Time absorption profiles at 508, 625, and 700 nm (black, red, gray, respectively) monitoring the ISC, the transduction of triplet excited state energy, and the triplet excited state decay of the photoexcited *N*-MFP with (c) **Rb** and (d) **NRb**.

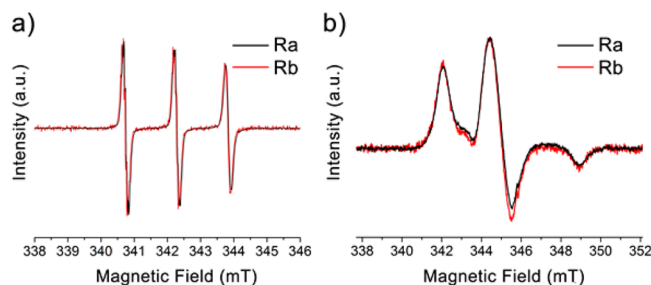


Figure 6. Steady-state CW EPR spectra of **Ra** (black trace) and **Rb** (red trace) at X-band (9.5 GHz) (a) obtained at 295 K with 0.005 mT modulation amplitude and (b) collected at 85 K with 0.02 mT modulation amplitude.

mechanism that selectively populates the γ - and z -triplet sublevels.⁵⁶ In the TREPR spectra for **Ra** and **Rb** (Figures 7d,e), this signal is completely quenched, and a narrow,

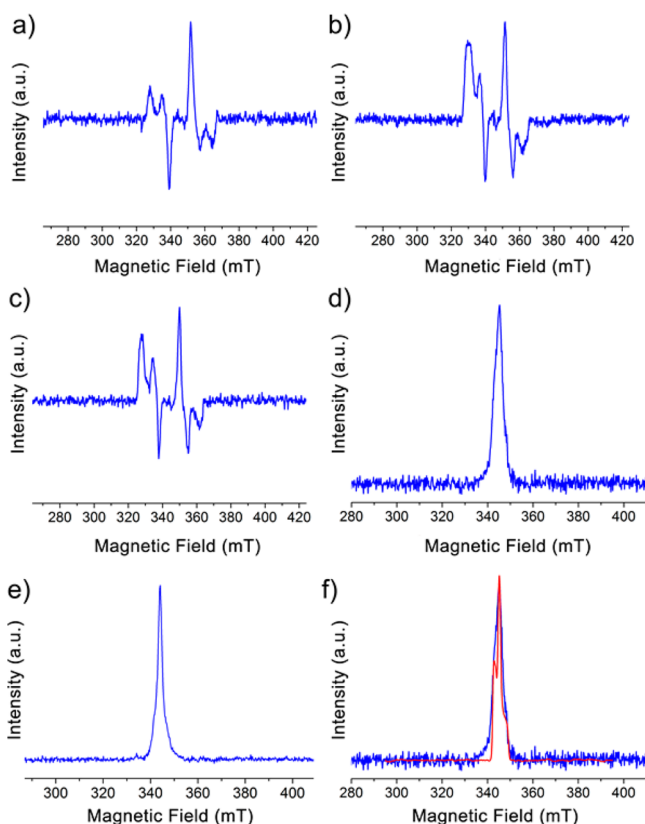


Figure 7. TREPR spectra obtained at 85 K. Field-swept, echo-detected (FS-ED) spectra of (a) NRa, (b) NRb, (c) TIPSPn were collected 3000 ns after a 7 ns, 590 nm laser pulse. Transient continuous wave (TCW) EPR spectra for (d) Ra and (e) Rb collected 2000 ns after a 7 ns, 590 nm laser pulse. (f) Overlay of the integrated TEMPO CW EPR spectrum (red) with the 400 ns time trace from the Ra TREPR spectrum (blue).

absorptively polarized signal is observed at $g \approx 2$. As shown in Figure 7f, the line shape of this signal matches that of the integrated steady-state CW EPR spectrum of the TEMPO radical itself indicating that a transient absorptive polarization of the nitroxide doublet state occurs by polarization transfer from the spin-polarized pentacene triplet state.

The appearance of spin polarization as a result of radical-triplet interactions has been studied in both strong and weak magnetic exchange coupling regimes and is commonly attributed to one of three possible mechanisms, namely the radical-triplet pair mechanism (RTPM),^{57–61} electron spin polarization transfer (ESPT),^{62–64} or the reversed quartet mechanism (RQM).⁶⁵ For RTPM, diffusional encounters between a radical and a spin-polarized triplet excited state in solution lead to a significant spin–spin exchange interaction between the two species. To this end, doublet and quartet excited states are generated, and in turn, their resulting polarization is determined by the sign of the exchange interaction between the photogenerated triplet and the radical, J_{TR} . For RQM, a fixed distance between the radical and the triplet excited state results in strong exchange interactions. This allows for mixing between doublet and quartet excited states and selective depletion of the doublet excited state to the ground state. Importantly, the conservation of spin multiplicity mandates a polarization inversion with time. Despite the fact that pentacene and TEMPO are covalently linked in these molecules, no quartet excited states are observed, and the

TEMPO polarization does not invert over time. Thus, these results are *not* consistent with the RTPM and RQM mechanisms. In contrast, the ESPT mechanism requires that the initially spin-polarized triplet excited state transfers its polarization to the radical by spin exchange, accompanied by quenching of the excited triplet state to the ground state singlet. The TREPR data in Figure 7 and the TA measurements both support the ESPT mechanism. Thus, the logical conclusion is that the ESPT mechanism (Figure 8) is responsible for the photophysical changes observed upon the covalent attachment of TEMPO to the pentacene framework via either a phenyl or a phenylethynyl spacer.

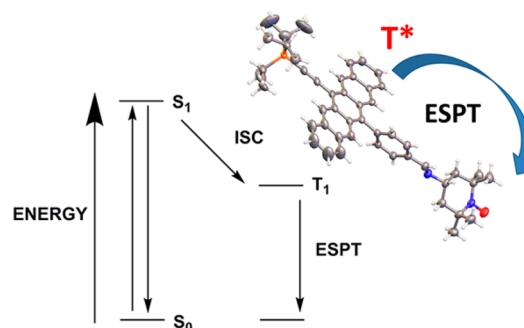


Figure 8. Jablonski diagram of the decay pathway for the pentacene radicals, as shown for Ra.

CONCLUSION

In summary, the first pentacene derivatives with a TEMPO stable free radical appended to the acene framework have been synthesized. Ultrafast TA experiments reveal spin–orbit ISC from the singlet excited state to the triplet excited state with no indication of enhanced intersystem crossing, while the triplet excited state is quenched by the TEMPO radical as a function of TEMPO-to-pentacene distance. TREPR experiments confirm that the pentacene triplet excited state is quenched by the electron spin polarization transfer mechanism indicating the TEMPO and pentacene are in the weak spin-exchange regime. We have successfully demonstrated that the extent of magnetic-exchange coupling between a stable free radical and excited state pentacene derivative can be modulated by spacial parameters dictated by the linker between these two groups. Furthermore, comparison of our results to those of Teki and co-workers in ref 31 shows that the extent of conjugation to the stable free radical also plays a role. These findings are important for the synthetic design of organic chromophores with the intention to impart selective control on the ISC process via magnetic-exchange coupling, i.e., how the excited state decay channels can be modulated through the choice of stable free radical as well as chromophore structure and geometry. Ultimately, switchable behavior might be envisioned through the design and synthesis of organic chromophores with differing stable free radicals that demonstrate varying magnetic-exchange coupling.

ASSOCIATED CONTENT

Supporting Information

Details of experimental procedures and characterization; crystallographic information in the form of CIF files; details of photophysical characterization. This material is available free of charge via the Internet at <http://pubs.acs.org>.

■ AUTHOR INFORMATION

Corresponding Authors

rik.tykwinski@fau.de

dirk.guldi@fau.de

m-wasielewski@northwestern.edu

Notes

The authors declare no competing financial interest.

■ ACKNOWLEDGMENTS

Funding is gratefully acknowledged from the “Solar Technologies go Hybrid” – an initiative of the Bavarian State Ministry for Science, Research and Art, the “Excellence Initiative” supporting the Cluster of Excellence “Engineering of Advanced Materials” (www.eam.uni-erlangen.de), and the Emerging Fields initiative “Singlet Fission”, supported by FAU. Work at Northwestern was supported by National Science Foundation Grant No. CHE-1266201.

■ REFERENCES

- (1) Ye, Q.; Chi, C. *Chem. Mater.* **2014**, *26*, 4046.
- (2) Anthony, J. E. *Angew. Chem., Int. Ed.* **2008**, *47*, 452.
- (3) Bendikov, M.; Wudl, F.; Perepichka, D. F. *Chem. Rev.* **2004**, *104*, 4891.
- (4) Murphy, A. R.; Fréchet, J. M. J. *Chem. Rev.* **2007**, *107*, 1066.
- (5) Tönshoff, C.; Bettinger, H. F. *Angew. Chem., Int. Ed.* **2010**, *49*, 4125.
- (6) Einholz, R.; Bettinger, H. F. *Angew. Chem., Int. Ed.* **2013**, *52*, 9818.
- (7) Kaur, I.; Jazdzzyk, M.; Stein, N. N.; Prusevich, P.; Miller, G. P. *J. Am. Chem. Soc.* **2010**, *132*, 1261.
- (8) Lee, J.; Bruzek, M. J.; Thompson, N. J.; Sfeir, M. Y.; Anthony, J. E.; Baldo, M. A. *Adv. Mater.* **2013**, *25*, 1445.
- (9) Chun, D.; Cheng, Y.; Wudl, F. *Angew. Chem., Int. Ed.* **2008**, *47*, 8380.
- (10) Qu, H.; Chi, C. *Org. Lett.* **2010**, *12*, 3360.
- (11) Kaur, I.; Stein, N. N.; Kopreski, R. P.; Miller, G. P. *J. Am. Chem. Soc.* **2009**, *131*, 3424.
- (12) Purushothaman, B.; Bruzek, M.; Parkin, S. R.; Miller, A.-F.; Anthony, J. E. *Angew. Chem., Int. Ed.* **2011**, *50*, 7013.
- (13) Mondal, R.; Tönshoff, C.; Khon, D.; Neckers, D. C.; Bettinger, H. F. *J. Am. Chem. Soc.* **2009**, *131*, 14281.
- (14) Sun, Z.; Wu, J. *J. Mater. Chem.* **2012**, *22*, 4151.
- (15) Walker, B. J.; Musser, A. J.; Beljonne, D.; Friend, R. H. *Nat. Chem.* **2013**, *5*, 1019.
- (16) Smith, M. B.; Michl, J. *Chem. Rev.* **2010**, *110*, 6891.
- (17) Smith, M. B.; Michl, J. *Annu. Rev. Phys. Chem.* **2013**, *64*, 361.
- (18) Lehnerr, D.; Tykwinski, R. R. *Aust. J. Chem.* **2011**, *64*, 919.
- (19) Pramanik, C.; Miller, G. P. *Molecules* **2012**, *17*, 4625.
- (20) Okamoto, T.; Bao, Z. *J. Am. Chem. Soc.* **2007**, *129*, 10308.
- (21) Lehnerr, D.; Murray, A.; McDonald, R.; Tykwinski, R. R. *Angew. Chem., Int. Ed.* **2010**, *49*, 6190.
- (22) Lehnerr, D.; Tykwinski, R. R. *Materials* **2010**, *3*, 2772.
- (23) Anthony, J. E. *Chem. Rev.* **2006**, *106*, 5028.
- (24) Anthony, J. E.; Brooks, J. S.; Eaton, D. L.; Parkin, S. R. *J. Am. Chem. Soc.* **2001**, *123*, 9482.
- (25) Northrop, B. H.; Houk, K. N.; Maliakal, A. *Photochem. Photobiol. Sci.* **2008**, *7*, 1463.
- (26) Naab, B. D.; Himmelberger, S.; Diao, Y.; Vandewal, K.; Wei, P.; Lussem, B.; Salleo, A.; Bao, Z. *Adv. Mater.* **2013**, *25*, 4663.
- (27) Brown, R.; Wrachtrup, J.; Orrit, M.; Bernard, J.; von Borczyskowski, C. *J. Chem. Phys.* **1994**, *100*, 7182.
- (28) Yu, H.-L.; Lin, T.-S.; Weissman, S. I.; Sloop, D. J. *J. Chem. Phys.* **1984**, *80*, 102.
- (29) Colvin, M. T.; Giacobbe, E. M.; Cohen, B.; Miura, T.; Scott, A. M.; Wasielewski, M. R. *J. Phys. Chem. A* **2010**, *114*, 1741.
- (30) Buchachenko, A. L.; Berdinsky, V. L. *Chem. Rev.* **2002**, *102*, 603.
- (31) Ito, A.; Shimizu, A.; Kishida, N.; Kawanaka, Y.; Kosumi, D.; Hashimoto, H.; Teki, Y. *Angew. Chem., Int. Ed.* **2014**, *53*, 1.
- (32) Kawanaka, Y.; Shimizu, A.; Shinada, T.; Tanaka, R.; Teki, Y. *Angew. Chem., Int. Ed.* **2013**, *52*, 6643.
- (33) van der Linden, M.; Borsboom, J.; Kaspersen, F.; Kemperman, G. *Eur. J. Org. Chem.* **2008**, 2989.
- (34) Komeyama, K.; Sasayama, D.; Kawabata, T.; Takehira, K.; Takaki, K. *Chem. Commun.* **2005**, 634.
- (35) Lehnerr, D.; McDonald, R.; Tykwinski, R. R. *Org. Lett.* **2008**, *10*, 4163.
- (36) Lehnerr, D.; Gao, J.; Hegmann, F. A.; Tykwinski, R. R. *Org. Lett.* **2008**, *10*, 4779.
- (37) Thorand, S.; Krause, N. *J. Org. Chem.* **1998**, *63*, 8551.
- (38) Xu, H.-D.; Zhang, R.-W.; Li, X.; Huang, S.; Tang, W.; Hu, W.-H. *Org. Lett.* **2013**, *15*, 840.
- (39) Kuramochi, Y.; Sandanayaka, A. S. D.; Satake, A.; Araki, Y.; Ogawa, K.; Ito, O.; Kobuke, Y. *Chem.—Eur. J.* **2009**, *15*, 2317.
- (40) Guzen, K. P.; Guarezemini, A. S.; Órfão, A. T. G.; Cella, R.; Pereira, C. M. P.; Stefani, H. A. *Tetrahedron Lett.* **2007**, *48*, 1845.
- (41) The structure of **4a** has been established by X-ray crystallography; see SI for details.
- (42) Ramanan, C.; Smeigh, A. L.; Anthony, J. E.; Marks, T. J.; Wasielewski, M. R. *J. Am. Chem. Soc.* **2012**, *134*, 386.
- (43) Confirmation for the triplet excited state comes from diffusion controlled triplet sensitization experiments, in which a fulleropyrrolidine (*N*-MFP) triplet excited state served as an energy donor state and **NRa** and **NRb** as energy acceptors. The correspondingly formed spectra for **NRa** and **NRb** are quantitative matches of the long-lived component. The structure of the fulleropyrrolidine *N*-MFP is given in the SI.
- (44) While Teki and co-workers reported SF in dilute solutions (10^{-4} M) of pentacene conjugated to a free radical (ref 31), the present study offers no evidence of singlet fission for solutions of either **Ra** or **Rb**. This can be explained by the weak magnetic exchange between the TEMPO radical and pentacene core, in addition to the low concentrations of the samples under which the TA measurements were performed. Friend and co-workers (ref 15) recently reported SF in concentrated solutions and concluded that SF is a bimolecular process governed by diffusion control in solution.
- (45) Eaton, S. S.; Eaton, G. R. *Electron Paramagn. Reson.* **2004**, *19*, 318.
- (46) Weil, J. A.; Bolton, J. R. *Electron Paramagnetic Resonance: Elementary Theory and Practical Applications*, 2nd ed.; Wiley: Hoboken, NJ, 2007.
- (47) The structure of TIPS pentacene is presented in the SI, and further details can be found in ref 24.
- (48) de Vries, H.; Wiersma, D. A. *J. Chem. Phys.* **1979**, *70*, 5807.
- (49) Eichhorn, T. R.; Haag, M.; van den Brandt, B.; Haulte, P.; Wenckebach, W. Th.; Jannin, S.; van der Klink, J. J.; Comment, A. J. *Magn. Reson.* **2013**, *234*, 58.
- (50) Kouskov, V.; Sloop, D. J.; Liu, S.-B.; Lin, T.-S. *J. Magn. Reson.* **1995**, *117*, 9.
- (51) van Strien, A. J.; Schmidt, J. *Chem. Phys. Lett.* **1980**, *70*, 513.
- (52) Sloop, D. J.; Yu, H.-L.; Lin, T.-S.; Weissman, S. I. *J. Chem. Phys.* **1981**, *75*, 3746.
- (53) Ong, J.-L.; Sloop, D. J.; Lin, T.-S. *Appl. Magn. Reson.* **1994**, *6*, 359.
- (54) Ong, J.-L.; Sloop, D. J.; Lin, T.-S. *J. Phys. Chem.* **1992**, *96*, 4762.
- (55) Lang, J.; Sloop, D. J.; Lin, T.-S. *J. Phys. Chem. A* **2007**, *111*, 4731.
- (56) Thurnauer, M. C.; Katz, J. J.; Norris, J. R. *Proc. Natl. Acad. Sci. U.S.A.* **1975**, *72*, 3270.
- (57) Fujisawa, J.; Ishii, K.; Ohba, Y.; Yamauchi, S.; Fuhs, M.; Möbius, K. *J. Phys. Chem. A* **1999**, *103*, 213.
- (58) Fujisawa, J.; Ishii, K.; Ohba, Y.; Yamauchi, S.; Fuhs, M.; Möbius, K. *J. Phys. Chem. A* **1997**, *101*, 5869.
- (59) Ishii, K.; Fujisawa, J.; Ohba, Y.; Yamauchi, S. *J. Am. Chem. Soc.* **1996**, *118*, 13079.
- (60) Blättler, C.; Jent, F.; Paul, H. *Chem. Phys. Lett.* **1990**, *166*, 375.

- (61) Corvaja, C.; Franco, L.; Toffoletti, A. *Appl. Magn. Reson.* **1994**, *7*, 257.
- (62) Blank, A.; Levanon, H. *J. Phys. Chem. A* **2001**, *105*, 4799.
- (63) Fujisawa, J.; Ishii, K.; Ohba, Y.; Iwaizumi, M.; Yamauchi, S. *J. Phys. Chem.* **1995**, *99*, 17082.
- (64) Fujisawa, J.; Ohba, Y.; Yamauchi, S. *J. Phys. Chem. A* **1997**, *101*, 434.
- (65) Rozenshtein, V.; Berg, A.; Stavitski, E.; Levanon, H.; Franco, L.; Corvaja, C. *J. Phys. Chem. A* **2005**, *109*, 11144.

■ NOTE ADDED AFTER ASAP PUBLICATION

Scheme 1 and References 21 and 36 have been updated. The revised version was re-posted on January 8, 2015.